ECMWF COPERNICUS | REPORT

Copernicus Europe's eyes on Earth

Copernicus Climate Change Service

Algorithm Theoretical Basis Document

Fundamental Climate Data Record of Microwave Humidity Sounder

Issued by: EUMETSAT

Date: 15/10/2019

REF.: C3S_311b Task 1.1 D1.1, D1.2, D1.3

European Commission

Copernicus Europe's eyes on Earth

IMPLEMENTED BY ECMWF

Algorithm Theoretical Basis Document (ATBD)

Fundamental Climate Data Record of Microwave Humidity Sounder

Timo Hanschmann
Viju John
Rob Roebeling
Mike Grant
Jörg Schulz

Date: 15/10/2019

REF.: C3S_311b Task 1.1 D1.1, D1.2, D1.3

Contents

List of Tables

List of Figures

1 Introduction

This ATBD presents the theoretical baseline description of the methods that are used for the generation of the microwave humidity sounder Fundamental Climate Data Records (FCDR). The microwave humidity sounder FCDRs contain consistently calibrated measurements of the 183 GHz channel measurements from the EUMETSAT Microwave Humidity Sounder (MHS), NOAA's Advanced Technology Microwave Sounder (ATMS), and the CMA MicroWave Humidity Sounders (MWHS/1 and 2), hereinafter referred to as Copernicus Climate Change Service (C3S) microwave sounder FCDRs. The C3S microwave sounder FCDRs have been generated within WP1, Task 1.1 in C3S_311b [AD1]) and built up on the methods developed within the European Union funded Horizon 2020 project *Fidelity and uncertainty in climate data records from Earth Observations (FIDUCEO)* (RD8, RD15, RD25).

1.1 Purpose of the document

The C3S microwave sounder FCDRs are described in three documents:

- Algorithm Theoretical Baseline Document (ATBD) (methods and algorithm description);
- Quality Evaluation Report (informs on the accuracy, precision, and stability of the product);
- User Guide (provides essential information for the user on the product definition, how to access and work with the data, and contains information on major limitations on the usage).

This document, the ATBD, provides the scientific basis of the algorithm by detailing the physical theory, mathematical procedures, and assumptions in deriving the FCDRs.

1.2 Structure of the document

This document is structured as follows:

- Section 1 provides an introduction;
- Section 2 presents an overview of the instruments and an introduction on metrological concepts;
- Section 3 provides a description of the algorithm;
- Section 4 describes the processing;
- Section 5 briefly introduces the measures for validation;
- Section 6 summarises constraints, limitations, and assumptions;
- Appendix A provides further information on the data processing.

1.3 Applicable Documents

AD1.	C3S Implementation Plan 2016-2021 EUMETSAT-D9_1_v1_0

1.4 Reference Documents

RD1.	NWP SAF, AAPP DOCUMENTATION - SCIENTIFIC DESCRIPTION, V8.0, 2017
RD2.	J. Bucher, "the Metrology Handbook 2nd edition", ASQ Quality Press, 2012 (ISBN: 978-0-87389-838-6)

RD3.	Product User Guide Fundamental Climate Data Record of Microwave Humidity Sounder, 2019, C3S_311b Task 1.1 D1.1, D1.2, D1.3
RD4.	Validation report for the Fundamental Climate Data Record of Microwave Humidity Sounder, 2019, C3S_311b Task 1.1 D1.1, D1.2, D1.3
RD5.	M. Dowell, P. Lecomte, R. Husband, J. Schulz, T. Mohr, Y. Tahara, R. Eckman, E. Lindstrom, C. Wooldridge, S. Hilding, J.Bates, B. Ryan, J. Lafeuille, and S. Bojinski, 2013: Strategy Towards an Architecture for Climate Monitoring from Space. Pp. 39.
RD6.	EUMETSAT, MHS Level 1 Product Generation Specification (EUM.EPS.SYS.SPE.990006), Version 6.0
RD7.	Hans, I., Burgdorf, M., John, V. O., Mittaz, J., and Buehler, S. A.: Noise performance of microwave humidity sounders over their lifetime, Atmos. Meas. Tech., 10, 4927-4945, https://doi.org/10.5194/amt-10-4927-2017, 2017
RD8.	Hans, I.; Burgdorf, M.; Buehler, S.A.; Prange, M.; Lang, T.; John, V.O. An Uncertainty Quantified Fundamental Climate Data Record for Microwave Humidity Sounders. *Remote Sens.* 2019, *11*, 548.
RD9.	NOAA KLM user's guide, 1999, U.S. Dept. of Commerce, National Oceanic and Atmospheric Administration, National Environmental Satellite, Data, and Information Service, National Climatic Data Center, Climate Services Division, Satellite Services Branch, http://webapp1.dlib.indiana.edu/virtual_disk_library/index.cgi/2790181/FID3711/klm/index.htm
RD10.	H. Jieying, Z. Shengwei and W. Zhenzhan, "Advanced Microwave Atmospheric Sounder (AMAS) Channel Specifications and T/V Calibration Results on FY-3C Satellite," in *IEEE Transactions on Geoscience and Remote Sensing*, vol. 53, no. 1, pp. 481-493, Jan. 2015. doi: 10.1109/TGRS.2014.2324173
RD11.	S. Gu, Y. Guo, Z. Wang and N. Lu, "Calibration Analyses for Sounding Channels of MWHS Onboard FY-3A," in *IEEE Transactions on Geoscience and Remote Sensing*, vol. 50, no. 12, pp. 4885-4891, Dec. 2012. doi: 10.1109/TGRS.2012.2214391
RD12.	Gu Songyan, Wang Zhenzhan,Li Jing,Zhang Shengwei and Zhang Li, "FY-3A/MWHS data calibration and validation analysis", Strategic Study of Chinese Academy of Engineering,2013,15(7):92-100.
RD13.	GUM (2008): "JCGM 100:2008 Evaluation of measurement data –Guide to the expression of uncertainty in measurement", Report, http://www.bipm.org/en/publications/guides
RD14.	Lambrigtsen, B.H., Algorithm Theoretical Basis Document – NASA L1B: Advanced Technology Microwave Sounder, Version 1, July 2014

RD15.	Merchant, C.J.; Holl, G.; Mittaz, J.P.D.; Woolliams, E.R. "Radiance Uncertainty Characterisation to Facilitate Climate Data Record Creation.", Remote Sens. 2019, 11, 474.
RD16.	Monarrez, Ruth, Data Product User Guide for Suomi-National Polar-Orbiting Partnership (S-NPP) Sounder Science Investigator-led Processing System (SIPS) Advanced Technology Microwave Sounder (ATMS) Level 1B Products, Product Version 2.0, 07/2018
RD17.	M. Schreier, B. Lambrigtsen, E. Fetzer, " Advanced Technology Microwave Sounder (ATMS) Assessment Report for Suomi National Polar-orbiting Partnership (SNPP) Sounder Science Investigator-led Processing System (SIPS) Data Level 1", 2018, NASA JPL
RD18.	M. Tian, X. Zou and F. Weng, "Use of Allan Deviation for Characterizing Satellite Microwave Sounder Noise Equivalent Differential Temperature (NEDT)," in *IEEE Geoscience and Remote Sensing Letters*, vol. 12, no. 12, pp. 2477-2480, Dec. 2015. doi: 10.1109/LGRS.2015.2485945
RD19.	Z. Wang, J. Li, S. Zhang and Y. Li, "Prelaunch Calibration of Microwave Humidity Sounder on China's FY-3A Meteorological Satellite," in IEEE Geoscience and Remote Sensing Letters, vol. 8, no. 1, pp. 29-33, Jan. 2011. doi: 10.1109/LGRS.2010.2050676
RD20.	Wang Zhenzhan, Zhang Shengwei and Li Jing, "Thermal/vacuum calibration of microwave humidity sounder on FY-3B satellite",Strategic Study of Chinese Academy of Engineering,2013,15(10):33-46.
RD21.	Emma R Woolliams *et al* 2018 *J. Phys.: Conf. Ser.* **972** 012003
RD22.	VIM (2008): "JCGM 200:2008 International vocabulary of metrology -basic and general concepts and associated terms", http://www.bipm.org/en/publications/guides
RD23.	FIDUCEO (2017): "D2.2(Microwave): Report on the MW FCDR: Uncertainty"
RD24.	WMO Data processing levels, http://www.wmo.int/pages/prog/sat/dataandproducts_en.php (assessed on 25.06.2019)
RD25.	Mittaz, J., Merchant, C. J. and Woolliams, E. R. (2019) Applying principles of metrology to historical Earth observations from satellites. Metrologia, 56 (3). ISSN 0026-1394, doi: https://doi.org/10.1088/1681-7575/ab1705

1.5 Acronyms

The following table lists the description for all acronyms used in this document.

Table 1: Definitions of all acronyms used in this document.

Abbreviation	Description
AAPP	ATOVS and AVHRR Pre-processing Package
ACDD	Attribute Convention on Data Discovery
AMSU	Advanced Microwave Sounding Unit
APC	Antenna Pattern Correction
ATBD	Algorithm Theoretical Basis Document
ATMS	Advanced Technology Microwave Sounder
BIPM	International Bureau of Weights and Measures
C3S	Copernicus Climate Change Service
CLASS	Comprehensive Large Array-data Stewardship System
DSV	Deep Space View
ECMWF	European Centre for Medium-range Weather Forecast
FCDR	Fundamental Climate Data Record
FIDUCEO	Fidelity and uncertainty in climate data records from Earth Observations
FY	Feng-Yun
GCMD	Global Change Master Directory
GUM	Guide to the expression of uncertainty in measurement
HDF	Hierarchical Data Format
IFOV	Instantaneous Field Of View
KLM	3rd generation of NOAA satellites
LO	Local Oscillator
LSB	Lower side band
Metop	Meteorological Operational Satellite
MHS	Microwave Humidity Sounder
MWHS	MicroWave Humidity Sounder
NASA/JPL	National Aeronautics and Space Administration / Jet Propulsion Laboratory
NRT	Near-Real-Time
NOAA	National Oceanic and Atmospheric Administration
OBCT	On-Board Calibration Target
PRT	platinum resistance thermometer
RFI	RadioFrequencyInterference
SAPHIR	Sondeur Atmosphérique du Profil d'Humidité Intertropical par Radiométrie
SNPP	Suomi National Polar-orbiting Partnership
SSP	Sub Satellite Point
USB	Upper side band
VIM	vocabulary of metrology

1.6 Symbols

The following table lists the description for all mathematical symbols used in this document.

Table 2 Definitions of all symbols used in this document.

Abbreviation	Description
L	Spectral radiance
T or T_{BT}	Brightness temperature
$T_{antenna}$	Antenna temperature
T_C	Cold target temperature
T_W	Warm target temperature
T_{linear}	Earth view temperature after linear calibration
T_{nl}	Earth view temperature after non-linearity correction
u	Non-linearity coefficient
u_1	First non-linearity coefficient for MWHS/1 on board of FY-3A
u_2	Second non-linearity coefficient for MWHS/1 on board of FY-3A
u_3	Third non-linearity coefficient for MWHS/1 on board of FY-3A
U	uncertainty
v_s	Measured radio frequency
v_{LO}	Frequency of the local oscillator
v_{IF}	Intermediate Frequency
$C_{earthview}$	Earth view counts
C_{OBCT}	On board calibration target counts
C_{DSV}	Deep space view counts
L_{DSV}	Deep space view radiance ,as observed by the instrument in a specific channel
L_{OBCT}	On board calibration target ,as observed by the instrument in a specific channel
L_{ME}	Measured earth radiance
L_E	Earth view radiance after applying the APC
g_E	Portion of FOV from the earth as used in MHS APC
g_P	Portion of FOV from the platform as used in MHS APC
g_S	Portion of FOV from the space as used in MHS APC
ΔL_{nl}	Non-linearity correction term
ΔT_{nl}	Non-linearity correction term as used for MHWS/1 on FY-3B
G	Instrument gain
AL	Allan deviation
W	Weighting matrix
C_{QC}	Quality controlled counts
A	Offset of the band correction coefficient
B	Slope of the band correction coefficient
C_1	First radiation constant
C_2	Second radiation constant
h	Planck constant
c	Speed of light
k_B	Boltzmann constant
ME	Measurement equation

1.7 Document Change Record

Version	Date	Document Number	Changes
1.0	15.10.2019	C3S_311b Task 1.1 D1.1, D1.2, D1.3	First version

1.8 Definitions

The following definitions are used throughout the document.

Data levels (RD24):

- **Level 1A:** Instrument counts with geolocation and calibration information attached but not applied
- **Level 1B:** Geolocation and calibration information applied to the instrument counts
- **Level 1C:** Instrument specific. For example, level 1b data converted to Brightness Temperature

Products types:

- **Operational data:** Level 1 data provided by an institution who is operating the sensor in space and provides data in near real time.
- **Fundamental Climate Data Record** [RD5]: The term FCDR denotes a well-characterised, long-term data record, usually involving a series of instruments, with potentially changing measurement approaches, but with overlaps and calibrations sufficient to allow the generation of products that are accurate and stable, in both space and time, to support climate applications. FCDRs are typically calibrated radiances, brightness temperatures, backscatter of active instruments, or radio occultation bending angles. FCDRs also include the ancillary data used to calibrate them. The term FCDR has been adopted by GCOS and can be considered as an international consensus definition.

2 Background information

2.1 Satellite instruments

The algorithm, presented in this ATBD, has been used to process data of microwave humidity sounder instruments measuring around the 183.31 GHz water vapour absorption band. The current version of the algorithm is designed to produce:

- the 2nd EUMETSAT release of the MHS FCDR;
- the 1st EUMETSAT release of the MWHS/1 FCDR;
- the 1st EUMETSAT release of the MWHS/2 FCDR;
- the 1st EUMETSAT release of the ATMS FCDR.

The MHS, MWHS/1, MWHS/2, and ATMS instruments are or were operated on different sun-synchronous, polar orbiting operational meteorological satellites at different periods:

- MHS on board of Metop A: 2006 – present
- MHS on board of Metop B: 2013 – present
- MWHS/1 on board of FY-3A: 2008 – 2014
- MWHS/1 on board of FY-3B: 2010 - present
- MWHS/2 on board of FY-3C: 2013 - present
- ATMS on board of S-NPP: 2011 - present

These satellites are orbiting the earth 14.2 times a day about 830km above the ground. Each instrument is a cross track scanner, with slightly varying swath width (2310km – 2660km). The field of view of each observation is 1.1°, which results in a nadir IFOV size of about 16 km (see Table 3).

The instruments mostly provide two passbands around the central frequency. This is well described in [RD23]. Below the most relevant information is presented:

- The microwave radiometers are heterodyne receivers, where the received radio frequency v_s is down converted to a lower intermediate frequency v_{IF} with a local oscillator (LO) at a specified and precisely controlled frequency v_{LO} and then amplified and filtered. The output at a frequency v_{IF} may be produced by a signal at either of two frequencies: $v_S = v_{LO} \pm v_{IF}$.

- For a given LO frequency, a mixer which produces output over the intermediate frequency range from v_{min} to v_{max} will therefore respond to input signals in the range from $v_{LO} + v_{min}$ to $v_{LO} + v_{max}$ and to signals in the range from $v_{LO} - v_{max}$ to $v_{LO} - v_{min}$. There are two bands of receivable signal frequencies, placed on either side of the LO frequency.

- The band from $v_{LO} + v_{min}$ to $v_{LO} + v_{max}$ is conventionally referred to as the Upper Side Band (USB). The band from $v_{LO} - v_{max}$ to $v_{LO} - v_{min}$ is referred to as the Lower Side Band (LSB). A receiver system, which responds to both of them, is called a double-sideband receiver. AMSU-B channels 3-5 are examples for channels that are configured for double-sideband operation. The gain transfer functions, i.e. the equivalent of the relative spectral response functions of instruments operating at optical wavelengths, of the LSB and the USB are mirror

images, i.e., their values are the same for $v_{LO} + v$ and $v_{LO} - v$. They are known from tests on ground.

Table 3 Overview on the characteristics of the instruments included in the FCDR.

characteristic	MHS	MWHS/1	MWHS/2	ATMS
# channels	5	5	16	21
# channels at 183.31 GHz	3	3	5	5
FOVs per scanline	90	98	98	96
FOV size at SSP [km]	16	16	16	16
Swath [km]	2310	2660	2660	2580

The channels around 183.31 GHz provide information from two sidebands, the USB and LSB, which have varying bandwidths. Together with their spectral distance to the central frequency, Table 4 to Table 7 lists the channels per instrument (only the channels printed in black are considered for the FCDRs). There are only minor differences between the instruments channels, which are the channel polarisation and the channel bandwidth. MHS is distinct, as it only provides the USB for the channel 5 at 190.31 GHz.

Table 4 Spectral characteristics of the MHS instrument

Channel	Central frequency [GHz]	Bandwidth [MHz]	Polarisation
1	89	2800	V
2	157	2800	V
3	183.31±1.0	1000	H
4	183.31±3.0	2000	H
5	190.31	2200	V

Table 5 Spectral characteristics of the MWHS/1 instrument.

Channel	Central frequency [GHz]	Bandwidth [MHz]	Polarisation
1	150	1001.46	H
2	150	987.08	V
3	183.31±1.0	480.77	V
4	183.31±3.0	1033.65	V
5	183.31±7.0	2186.40	V

Table 6 Spectral characteristics of the MWHS/2 instrument.

Channel	Central frequency [GHz]	Bandwidth [MHz]	Polarisation
1	89	1500	V
2	118.75±0.08	20	H
3	118.75±0.2	100	H
4	118.75±0.3	165	H
5	118.75±0.8	200	H
6	118.75±1.1	200	H
7	118.75±2.5	200	H
8	118.75±3.0	1000	H
9	118.75±5.0	2000	H
10	150	1500	V
11	183.31±1.0	500	H
12	183.31±1.8	700	H
13	183.31±3.0	1000	H

Channel	Central frequency [GHz]	Bandwidth [MHz]	Polarisation
14	183.31±4.5	2000	H
15	183.31±7.0	2000	H

Table 7 Spectral characteristics of the ATMS instrument.

Channel	Central frequency [GHz]	Bandwidth [MHz]	Polarisation
1	23.8	270	QV
2	31.4	180	QV
3	50.3	180	QH
4	51.76	400	QH
5	52.8	400	QH
6	53.596±0.115	170	QH
7	54.4	400	QH
8	54.94	400	QH
9	55.5	330	QH
10	57.290344 (X)	330	QH
11	X±0.217	78	QH
12	X±0.3222±0.048	36	QH
13	X±0.3222±0.022	16	QH
14	X±0.3222±0.010	8	QH
15	X±0.3222±0.0045	3	QH
16	88.2	2000	QV
17	165.5	3000	QH
18	183.31±7.0	2000	QH
19	183.31±4.5	2000	QH
20	183.31±3.0	1000	QH
21	183.31±1.8	1000	QH
22	183.31±1.0	500	QH

2.2 The basic calibration concept

The microwave humidity sounding instruments measure radiation at each earth view in an across track scan and store them as count values ($C_{Earthview}$). Additionally, two calibration targets, the deep space view (DSV) and the on-board warm calibration target (OBCT), are measured three to four times in each scanline and their measurements are stored as well as count values (C_{DSV} and C_{OBCT}). The temperature of the on-board calibration target is stabilised and measured by about five platinum resistance thermometers (PRTs). These temperature measurements are converted to the radiance, which the target emits (L_{OBCT}) and the instrument would measure in each channel. Also, the space temperature of 2.73K, the cosmic background temperature, which the instrument would measure in each channel (L_{DSV}) is converted into radiance. With the known calibration target temperatures and the measured calibration counts, a two-point linear calibration equation is derived, which converts the measured Earth view counts x into the earth view radiance.

Section 3.1 introduces the applied measurement equation in more detail and adds further necessary terms, such as the non-linearity correction.

2.3 Uncertainty Characterisation

As mentioned above, for the C3S microwave sounder FCDRs methodology developed within FIDUCEO is applied. In FIDUCEO and C3S, the recalibrated brightness temperatures are delivered with associated metrologically traceable uncertainty estimates.

Characterising measurements in a metrological sense means that, firstly, any calibration of a measurement can be traced back to a reference standard, secondly, any quantity is given in a defined unit, and thirdly, the measurement is only complete with an associated uncertainty estimate because the of a measurand is by nature indeterminate. According to the metrological principles, this is achieved by:

1) Definition of the measurand and the measurement model;
2) Definition of the input quantities;
3) Determination of uncertainty estimates for the input quantities;
4) Propagation of uncertainty estimates to a combined standard uncertainty;
5) Calibration of the measurement to the measurement standard;
6) Relating the calibration to a measurement reference, optimally in base units;
7) Provision of traceability in the measurement, its uncertainty, and calibration.

The metrological methodology is mainly described by two overarching documents, i) the "Evaluation of measurement data — Guide to the expression of uncertainty in measurement" (GUM) [RD13] and ii) the "International vocabulary of metrology – Basic and general concepts and associated terms" (VIM) [RD22]. The GUM defines the measurement concepts and the measurement uncertainties. The VIM is a vocabulary, defining all terms, which are used in metrology. Metrology clearly distinguishes between the measurement error and the measurement uncertainty (GUM). The measurement error is the difference between the measured quantity value and a true value of the measurand. The measurement uncertainty is a non-negative parameter, associated with the result of a measurement that characterizes the dispersion of the values that could reasonably be attributed to the measurand.

Since the true value of the measurand is unknown, the measurement error is unknown. However, by analysing the sources of errors in an EO measurement, the uncertainty in the measured value can be characterised. Estimating the uncertainty involves complex considerations, because any measurement is subject to several different sources of error, or 'effects' [RD25]. The measurement error should be divided into the random and the systematic error. Random errors are errors manifesting independence, i.e., error in one instance is in no way predictable from knowledge of the error in another instance. Systematic errors are those that could, in principle, be corrected if we had sufficient information to do so, that is, they arise from unknowns that could in principle be estimated rather than from chance processes.

FIDUCEO categorizes the errors into three: independent errors, structured errors, and common errors [RD25]. Independent errors arise from random effects causing errors that manifest independence between pixels, such that the error in one measurement is in no way predictable from knowledge of the error in another measurement, were that knowledge available. Independent errors therefore arise from random effects operating on a pixel level, the classic example being detector noise. Structured errors arise from effects that influence more than one measured value in the satellite image, but are not

in common across the whole image. The originating effect may be random or systematic (and acting on a subset of pixels), but in either case the resulting errors are not independent, and may even be perfectly correlated across the affected pixels. Since the sensitivity of different pixels/channels to the originating effect may differ, even if there is perfect error correlation, the error (and associated uncertainty) in the measured radiance can differ in magnitude. Structured errors are therefore complex, and, at the same time, important to understand, because their error correlation properties affect how uncertainty propagates to higher-level data. Common errors are constant (or nearly so) across the satellite image, and may be shared across the measured radiances for a significant proportion of a satellite mission. Common errors might typically be referred to as biases in the measured radiances. Effects such as the progressive degradation of a sensor operating in space mean that such biases may slowly change.

All sources of error in the measurement process need to be assessed, and the associated uncertainties need to be estimated and propagated to in the unit of the measurand, in this case brightness temperature. Uncertainties $U(x_i)$ are associated with the parameters x_i of each modelled effect from the measurement equation (there are N modelled effects). Furthermore, the sensitivity coefficients c_i for each effect were computed as the corresponding partial derivative of the measurement equation [RD8]. Finally, the resulting uncertainty on brightness temperature is obtained by applying the Law of Propagation of Uncertainties [GUM][RD25].

$$U_c(L) = \sqrt{\sum_{i=1}^{N} c_i^2 U^2(x_i)}, \text{ with} \qquad 2\text{-}1$$

U_c = combined uncertainty for a particular category, e.g., structured
U = uncertainty associated to an input quantity (or a single effect)
c = sensitivity coefficient
N = number of input quantities or effects
x = input quantity
L = measured radiance

If input quantities are significantly correlated, the correlation between the input quantities must be taken into account. This is done by adding the covariance (GUM, section 5.2.2; RD8, equation 9):

$$U_c(L) = \sqrt{\sum_{i=1}^{N} c_i^2 u^2(x_i) + 2\sum_{i=1}^{N-1}\sum_{j=i+1}^{N} c_i c_j u(x_i, x_j)}. \qquad 2\text{-}2$$

Here $U(x_i, x_j)$ is the estimated covariance associated with the input quantities x_i and x_j. Once uncorrelated input quantities are propagated by the first equation and correlated input quantities are propagated with the second equation, the independent and structured uncertainty of the measurement is described. Both can be specified separately or combined via the root-sum-squared method to U_{tot}:

$$U_{tot} = \sqrt{U_{ind}^2 + U_{str}^2 + +U_{com}^2} \qquad 2\text{-}3$$

Where U_{ind} is the Uncertainty estimate of independent effects, U_{str} of structured effects, and U_{com} of common effects.

3 Algorithm physical basis

This section describes the physical basis of the algorithm, which is based on the FIDUCEO methodology [RD7], [RD8] and [RD23]. Firstly, the measurement model is introduced and the differences in its application to the different instruments is explained. Secondly, the effects causing errors in the measurements are introduced, and it is explained how they are included in the measurement model. This includes uncertainty estimates and their propagation to combined uncertainties as described in section 2.3. Thirdly, the quality control of the measurements is described.

This ATBD makes use of existing ATBDs and publications that provide comprehensive information on the instruments and the individual calibration principles applied. The most important references for each instruments are listed here for convenience:

- MHS: [RD1], [RD6], [RD7], [RD8], [RD9], [RD23];
- ATMS: [RD14], [RD16], [RD17];
- MWHS/1: [RD11], [RD12], [RD19], [RD20];
- MWHS/2: [RD10].

3.1 The measurement equation

Each instrument requires a slightly different treatment of the calibration process, forced by available calibration constants, which have been provided by the instrument operators. However, the calibration process, summarised by the measurement equation, is homogenised as far as possible across the instruments. Remaining differences are explained below.

Generally, two kinds of measurement equations are applied: The calibration performed in radiance (L) for MHS and MWHS, and the calibration performed in temperature (T) for ATMS.

The calibration in radiance is based on the two-point calibration, introduced in section 2.2, including further corrections, resulting in L_{ME}:

$$L_{ME} = L_{OBCT} + \frac{L_{OBCT} - L_{DSV}}{\overline{C_{OBCT}} - \overline{C_{DSV}}} * (C_{earthview} - \overline{C_{OBCT}}) + \Delta L_{nl} + 0, \quad 3\text{-}1$$

where:

L_{ME}: measured Earth scene radiance;
L_{OBCT}: radiance emitted by the on-board calibration target (OBCT) determined from the OBCT temperature after bias correction;
L_{DSV}: radiance related to the cosmic background temperature after bias correction;
$\overline{C_{OBCT}}$: averaged measured count of the OBCT (see section 3.3);
$\overline{C_{DSV}}$: averaged measured count of the OBCT (see section 3.3);
$C_{earthview}$: measured count of the earth view pixel to be calibrated;
ΔL_{nl}: non-linear correction applied in an extra step;
$+0$: zero order term representing the extent to which this equation is an approximation [RD23].

The correction term for the detector non-linearity, ΔL_{nl}, is computed with:

$$\Delta L_{nl} = u * (C_{earthview} - \overline{C_{DSV}}) * (C_{earthview} - \overline{C_{OBCT}}) * \left(\frac{(L_{OBCT} - L_{DSV})}{(\overline{C_{OBCT}} - \overline{C_{DSV}})}\right)^2 \quad , \qquad 3\text{-}2$$

where u is the non-linearity correction coefficient that has been measured for each detector pre-launch and is provided by the instrument operator.

In a following step, the radiance, L_{ME}, is converted into the antenna temperature ($T_{antenna}$) by using the Planck law:

$$T_{antenna} = \frac{1}{B} * \left(\frac{c_2 * \nu}{\log(\frac{c_1 \nu^3}{L_{ME}} + 1)} - A\right), \qquad 3\text{-}3$$

where:

A and B:	the band correction coefficients for the specific channel;
$c_1 = 2 * h * c^2$:	the first radiation constant;
$c_2 = {h * c}/{k_B}$:	the second radiation constants;
c:	the speed of light;
h:	the Planck constant;
k_B:	the Boltzmann constant.

For MWHS/1 on-board of FY-3A the non-linearity correction is applied differently. In this case, the Planck law above is a function of the radiance from the linear calibration (as described in section 2.2). Further, the non-linearity coefficient for MWHS/1 on FY-3A is not provided as a single parameter, instead, the non-linearity correction is a quadratic correction resulting in a non-linearity correction term $\Delta T_{nl_{MWHS/FY3A}}$, which is added to the equation for $T_{antenna}$. The provided non-linearity coefficients, u_1, u_2, and u_3, are three coefficients in the quadratic correction. This is applied to the antenna temperature ($T_{antenna}$) as follows:

$$\Delta T_{nl_{MWHS/FY3A}} = \left(u_1 + u_2 * T_{antenna} + u_3 * T_{antenna}^2\right), \qquad 3\text{-}4$$

$$\text{with: } T_{antenna} = T_{antenna} + \Delta T_{nl_{MWHS/FY3A}}. \qquad 3\text{-}5$$

Side lobe effects in the field of view of the instrument antenna or its mirror affect antenna temperatures. The radiation is reflected from the satellite, instrument or space into the receiver. This radiation cannot be attributed to the radiation emitted by the Earth and its atmosphere. Therefore, this unwanted contribution must be removed from the antenna temperature. This is done by applying an antenna pattern correction (APC), which has been determined pre-launch. For MHS, it provides information on the portion in each field of view that sees the Earth (g_E), the instrument (g_P), and the space (g_S). For ATMS and MWHS, the APC are coefficients of a correction function. The application of the APC yields brightness temperature as a result.

For MHS, the APC is applied to the radiance (L_{ME}), before converting the radiance to the antenna temperature. The corrected Earth radiance is L_E:

$$L_E = \frac{1}{g_E} * (L_{ME} - (1 - g_E) * L_{DSV}) \qquad 3\text{-}6$$

Here, the g_E is the portion of the measured radiance coming from the Earth, defined by a value between 0 and 1. L_E is then used instead of L_{ME} in the Planck law, which in this case directly yields the brightness temperature.

For MWHS, the APC is provided as offset (APC_1) and slope (APC_2), applied to the antenna temperatures, yielding the brightness temperature (T_{BT}):

$$T_{BT} = APC_1 + APC_2 * T_{antenna} \quad \text{3-7}$$

For ATMS the calibration is performed directly in antenna temperature and the measurement equation is slightly different [RD16]. First, the calibration targets temperatures are computed. The cosmic background temperature of T=2.72548K is used as the cold calibration target temperature. For low temperatures and higher frequencies, as in this case, the Rayleigh-Jeans approximation for brightness temperatures breaks down. To account for this, the thermodynamic definition of the brightness temperature has to be used (for more information see [RD14], page 16-17). For the specific frequency, the cold calibration target temperature is given by

$$T_C = A + B\left(\frac{h*f}{k}\left(\frac{1}{e^{f*f/_{k*T}}} + 0.5\right) + dT_c\right), \quad \text{3-8}$$

with dT_c as the cold target bias.

The OBCT temperature (Tw) is computed by:

$$T_w = A + B(T_{OBCT} + dT_w)\,, \quad \text{3-9}$$

with dT_w as the warm target bias, which is determined during the pre-launch characterisation.

The antenna temperature, T_{linear}, based on the linear calibration, is computed by:

$$T_{linear} = T_w + (C_{earth} - \bar{C}_{OBCT}) * \frac{T_w - T_c}{\bar{C}_{OBCT} - \bar{C}_{DSV}}. \quad \text{3-10}$$

The non-linearity correction is computed and added to T_{linear}, which gives T_{nl} similar to $T_{antenna}$ above:

$$T_{nl} = T_{linear} + u * \left(1 - 4\left(\frac{T_{linear} - T_c}{T_w - T_c} - 0.5\right)^2\right). \quad \text{3-11}$$

As for the other instruments, in the last step the APC is applied:

$$T = T_{non-linear} - APC \quad \text{3-12}$$

The APC has been provided by NASA/JPL and might be different to the one applied at NOAA. Generally, it should be noted that the NASA calibration approach for ATMS differs from NOAA's approach and both NASA and NOAA have changed their approach over the lifetime of ATMS. More information are summarised in [RD17].

3.2 Use of calibration targets

Values from both calibration targets, the space and the OBCT measurements, are implemented following the FIDUCEO methodology, introduced in [RD8] and [RD23].

The space target is considered to be stable and does not require any further analysis, beside the conversion into the radiance or temperature the instrument would measure in a specific spectral channel.

The OBCT is temperature stabilised and its temperature is monitored by PRT measurements, equally distributed over the OBCT surface. Its temperature should only vary slowly during one orbit within a small temperature range. The PRT temperature measurements for each scanline are quality controlled and averaged. Then, these averaged temperatures are averaged over several scanlines to reduce the impact of noise. More details on the averaging is provided below in section 3.3.

The only exceptions in the processing of the OBCT are the MWHS/1 and MWHS/2 instruments. For these instruments, the single PRT measurements of the OBCT could not be decoded and the scanline averaged OBCT temperature, provided in the input files is used.

Based on the pre-launch tests, a calibration target temperature bias has been computed for each channel by the instrument operators, which is used to correct the calibration target temperatures. For ATMS this is included in the equations provided above, and for the other instruments, this is included in the conversion from the target temperature to radiance.

3.3 Processing of calibration measurements

The calibration target measurements are stored as counts (C_{DSV} and C_{OBCT}) and they are used in the measurement equation above as averaged counts. The averaging is performed according to the operational ATBDs over several scanlines considering a weighting function. This is required to make the calibration even more robust against undesired noise. For example, the striping noise, found in the ATMS data [RD17], is reduced. The averaging function is applied to the DSV and OBCT counts as well as the PRT temperatures of the OBCT that passed a quality test (see section 3.7) and it performs a multi scanline weighted mean for each scanline. The quality controlled PRT temperatures of each scanline are first averaged to one OBCT temperature per scanline. This weighted averaging is described by:

$$\bar{C} = \boldsymbol{W}^{-1} * {C_{QC}}^{-1} \,, \qquad 3\text{-}13$$

where $\mathbf{W}$ is the weighting matrix, C_{QC} is the quality-controlled counts, and $\bar{C}$ is the resulting averaged counts. $\mathbf{W}$ is applied as a matrix, defined as below, and C as a vector. The weighting coefficients, included in $\mathbf{W}$, are presented in Figure 1 for MHS and MWHS on the left side and for ATMS on the right side. According to the operational processing for ATMS [RD17] a 5 (channel 20 and 21) and 9 (channel 17, 18, 19, and 22) scanline box weighting is applied, which should reduce the striping noise in ATMS.

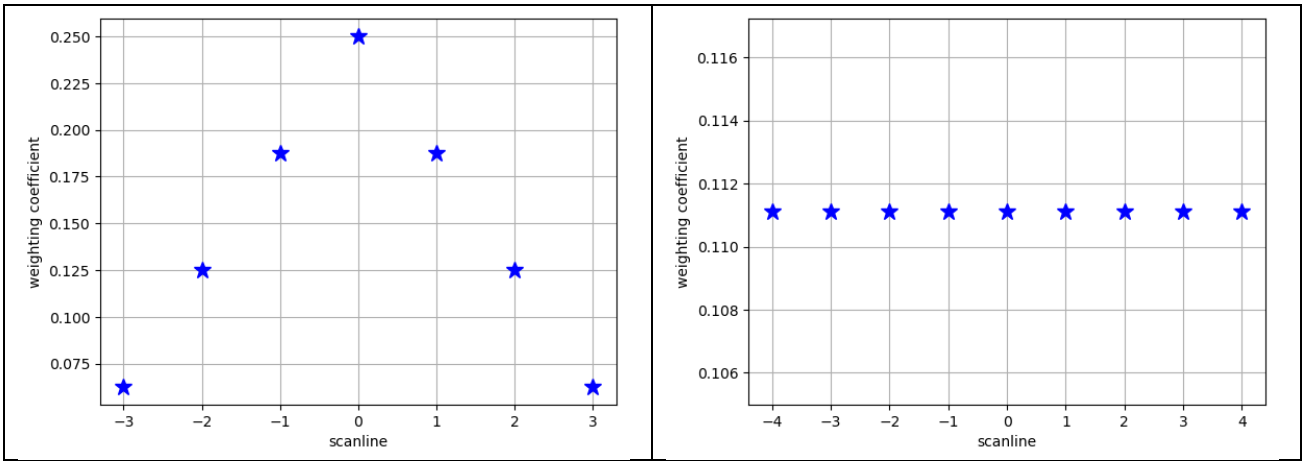

Figure 1 Weighting coefficients for the weighted average of calibration parameters. The left image shows the weighting function for the calibration of MHS and MWHS and the right for the calibration of ATMS.

The seven scanline weighted averaging for MHS and MWHS is performed according to [RD6]. Scanlines, which have been omitted from the processing due to not passing the quality control, are also excluded from this averaging. The weighting coefficients are corrected according to the number of omitted scanlines in the averaging window and the distance to the central scanline. This ensures that the sum of the weighting coefficients remain one.

Scanlines that do not provide any valid calibration information are re-filled, if possible, by including the median of the 10 closest surrounding averaged scanlines that passed the quality tests.

3.4 Uncertainty propagation

Uncertainty estimates are computed for each effect producing errors in the measurement. This follows the methodology developed within the FIDUCEO project [RD15, RD21]. Based on the correlation structure applied in FIDUCEO, the individual effect uncertainty estimates are propagated to three combined uncertainties described above.

The FIDUCEO project has identified the effects that are most relevant for the microwave sounding measurements [RD23]. The considered effects are:

- Uncertainty in the Earth counts
- Uncertainty in the DSV counts
- Uncertainty in the OBCT counts
- Uncertainty in the OBCT target temperatures
- Uncertainty from reflected / emitted radiation of the satellite platform

The following uncertainties are based on effects, which are related to coefficients for specific parts of the process outlined above. These are provided by the instrument operators and are assumed to not change over time:

- OBCT temperature - PRT bias
- Warm temperature bias uncertainty
- Cold temperature bias uncertainty

- Nonlinearity coefficient uncertainty
- Antenna correction coefficient uncertainty
- Uncertainties in the earth view antenna position
- Uncertainties in the DSV antenna position (only for MHS)
- Systematic uncertainty in the antenna position (only for MHS)

More information on the individual effects affecting the measurements are given in [RD23]. The computations of the associated uncertainty is described in section 3.5 and the propagation in section 3.6.

3.5 Compute calibration uncertainty

The uncertainty associated with the calibration counts and the OBCT target temperature is calculated as type A uncertainty (see section 2.3 for more information). The uncertainty of the calibration counts is computed over all counts (x) per scanline and over 300 scanlines, which pass the quality control, via the Allan deviation (AL) [RD18]:

$$AL = \sqrt{\frac{1}{2}(\overline{x_{i+1} - x_i})^2}. \quad 3\text{-}14$$

Similarly, the uncertainty of the OBCT target temperatures is computed via the Allan deviation over 300 scanlines, which is applied to quality controlled averaged PRT measurements in each scanline.

The uncertainty in the Earth count measurements is estimated by inserting the calibration count uncertainty in the measurement equation for the linear calibration for the calibration target temperatures and solving it:

$$\Delta_{X_{earth-view}} = U_{OBCT} + \frac{U_{OBCT} - U_{DSV}}{\overline{C_{OBCT}} - \overline{C_{DSV}}} * (C_{earthview} - \overline{C_{OBCT}}), \quad 3\text{-}15$$

where U_{OBCT} is the result from the Allan deviation applied to the OBCT counts and U_{DSV} from the Allan deviation applied to the DSV counts.

The sensitivity of the brightness temperature to the uncertainty of each effect varies. To consider this, the computed uncertainty, Δ_X, of a single effect, X, is multiplied with a sensitivity coefficient, $\frac{\partial L_E}{\partial X}$, which is the partial derivative of the measurement equation with respect to the effect. Further, the uncertainty is given in the same unit as the brightness temperature, i.e., Kelvin. Then, the uncertainty is multiplied by the derivative of the Planck function with respect to radiance ($\frac{\partial T}{\partial L}$), which gives the change in temperature T at the observed radiance L. The uncertainty that a single effect has on the resulting brightness temperature can be expressed as:

$$U_X = \frac{\partial T}{\partial L} * \frac{\partial L_E}{\partial X} * \Delta_X. \quad 3\text{-}16$$

3.6 Combination of uncertainties

The uncertainties are provided as independent, structured, and common uncertainty. Uncertainty is independent if it is uncorrelated to the uncertainty for any other measurements taken by the instrument. Uncertainty is structured when it is correlated in space and time. Within the FIDUCEO project, a spatial scale of 300 scanlines [RD7] has been evaluated to be useful for the computation of the structured uncertainty. Uncertainty is common if it appears in all measurements and during the entire lifetime of the instrument, e.g., by using the same calibration target for all measurements. More information on the different types of uncertainties can be found in the FIDCUEO project documentation [RD25].

The dominating effects contributing to the independent uncertainty estimate are:

- Measurement uncertainty in the Earth counts
- Uncertainty in the Earth view antenna position

The dominating effects contributing to structured uncertainty estimates are:

- Uncertainty in the DSV counts
- Uncertainty in the OBCT counts
- Uncertainty in the OBCT temperatures
- Uncertainty in the DSV antenna position (only for MHS)

. Common effects are generally addressed with pre-launch determined information. The dominating effects contributing to common uncertainty estimates are:

- OBCT temperature - PRT bias
- Warm temperature bias uncertainty
- Cold temperature bias uncertainty
- Nonlinearity coefficient uncertainty
- Polarisation correction coefficient uncertainty (only for MHS)
- Antenna correction coefficient uncertainty
- Uncertainty from reflected / emitted radiation of the platform
- Systematic uncertainty in the antenna position (only for MHS)

3.7 Quality control of the measurements

As mentioned above Earth view and calibration counts as well as the OBCT target temperature measurement are quality controlled before being used in the calibration process. This section outlines the applied quality control mechanisms, which are all of statistical nature.

Four statistical tests have been defined to filter observations with are not within the expected range or exhibit unexpected variation:

1. Threshold test
2. Median test
3. Min-max test
4. Test for identifying jumps and plateaus

For evaluating the quality of the DSV and OBCT calibration counts all four tests are applied. For the OBCT temperature, the third test is omitted, and for the Earth view counts, only the fourth test is applied.

The threshold tests, as defined in [RD1], prevents the use of counts and the OBCT temperature outside a predefined count limit in the further processing. The count limits are defined static over the whole lifetime.

The median test ensures that within each scanline only those calibration counts are used, which differ by less than 3 times the first guess count variation[1] from the scanline median of the calibration counts or OBCT temperature measurements.

The min-max test ensures that the difference between the lowest count minus the highest count within a scanline is lower than 5 times the first guess count variation. If this test fails, the quality of the whole scanline is flagged as bad.

The fourth test identifies possible jumps and plateaus in the time series (for the earth view counts, the time series considers all counts at one scan position). These are detected, when the scanline value changes by more than a pre-determined threshold. In this case, these scanlines are flagged as bad. Such scanlines are considered as if they were filled by the median count values of all valid data within the 10 surrounding scanlines as described above. The thresholds are being applied according to FIDUCEO [RD23].

For the DSV counts, additionally the angle between the DSV and the moon is computed. If the angle is below a certain threshold (2.5°), the DSV count is not used for the calibration.

[1] Defined as the Allan deviation over 300 scanlines without applying quality control. See also section A.1.

4 Data Processing

4.1 Processing scheme overview

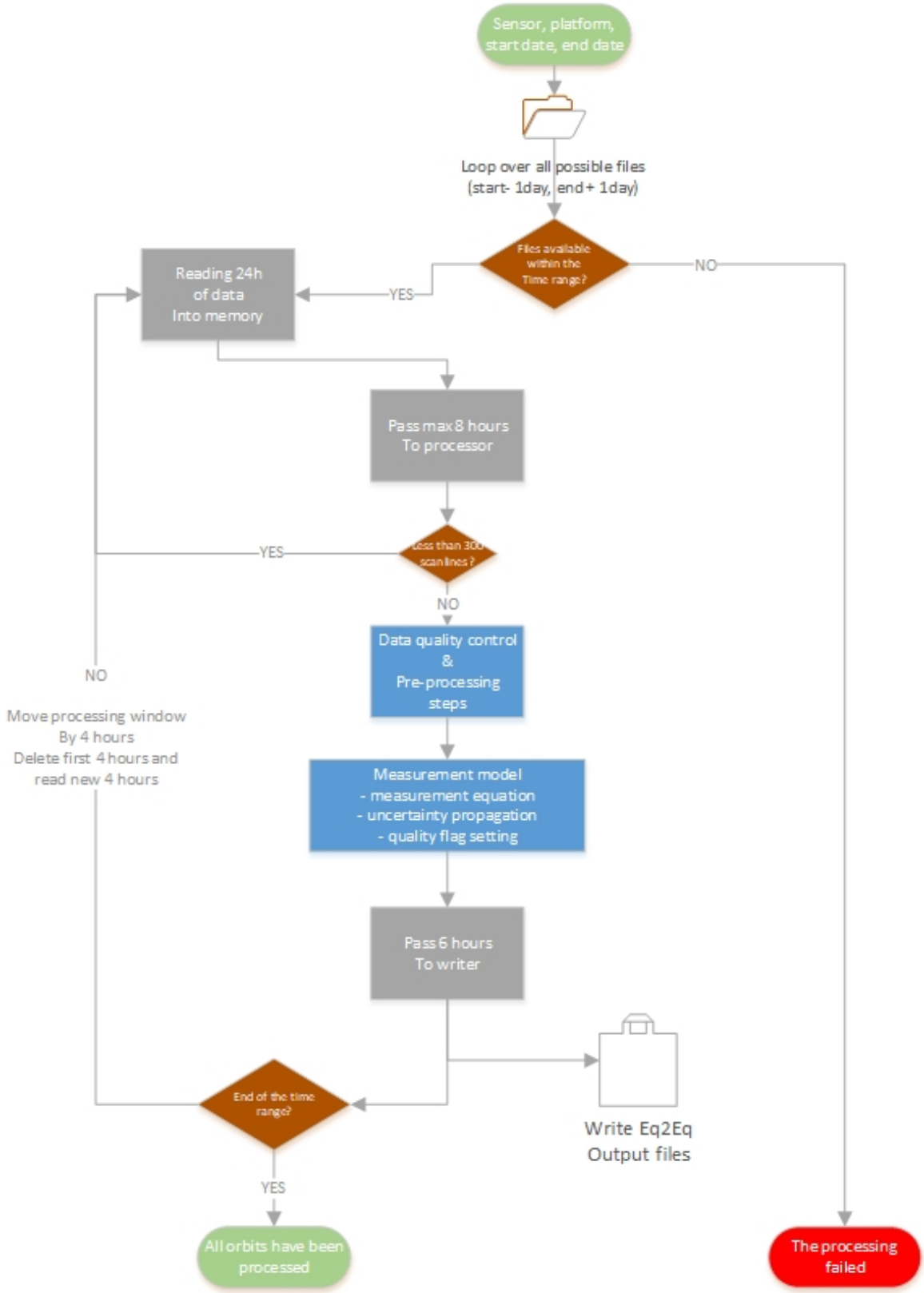

Figure 2: Overview of the processing scheme implemented for the C3S microwave sounder FCDRs. The output of the software are orbit files, which start and end at the equator (EQ2EQ).

The processing of the C3S microwave sounder FCDRs does not follow single-orbit-processing logic. Instead, it interprets data from polar orbiting satellites as continuous measurement stream that uses time as coordinate along which the processing is organised (Figure 2).
All observations over 24 hours are merged along the time axis. From this, the central 8 hours are processed. 8 hours was found to be an optimal compromise between processing speed and allocated memory. After processing, the central 6 hours are passed to the data-writing module. The two hours are skipped in order to avoid including data, which are affected by boundary effects. Boundary effects occur e.g. due to the 300 scanlines considered in the Allan deviation for the calibration parameter quality control. The writing module fragments the 6 hours of data into orbit files. Each orbit starts at the equator in the descending node and ends at the equator in the following descending node (EQ2EQ - files). Additional processing steps are provided in 6A.1

4.2 Algorithm input

The C3S microwave sounder FCDRs consist of data from different instruments, which are available in different data formats. Level 1a/1b data are used as input, which include instrument counts, calibration counts, viewing geometry information, and geolocation information. For MWHS/1, this information is stored with the calibrated brightness temperature in one level 1c file. The data formats differ between the agencies and range from NetCDF4, HDF5, to binary files. For each instrument, a dedicated data reading software element has been prepared that reads the data, decodes required coefficients, and merges all information into a common variable design, which interfaces with the upper level processing software module.

4.3 Algorithm output

The processed data are geographically split at the equator, from north to south, defining each orbit as covering from equator-to-equator. The output data format is NetCDF4 and includes brightness temperatures, uncertainty estimates and quality flags as well as geolocation and viewing geometry information. In addition, variable and global attributes in CF standard are provided within the output files. Detailed information on the quality flags can be found in 6A.2.

5 Algorithm validation

Product validation has been performed by comparison of the FCDR with:

- Other satellite data serving as reference, here SAPHIR;
- Operational brightness temperatures;
- Simulated brightness temperatures using ERA-5 as input.

The validation results by means described above are consistent and show improvements for the FCDR compared to the operational brightness temperatures. Further information is available in the Quality Evaluation Report [RD4].

6 Constraints, Limitations, and Assumptions

Resulting FCDRs have quality limitations due to insufficient information from data providers that are listed here to foster understanding of results:

- For the ATMS instrument, the processing at NASA/JPL has been applied. It is known, that the applied tests and corrections to the data differ to the operational processing at NOAA, which generate the ATMS SDR data files.
- For the MWHS/1 and MWHS/2 instrument, the OBCT temperature measurement of the single PRT sensor could not be converted from counts to Kelvin. Therefore, the quality control of the PRT measurements, removal of possible outliers, and the assessment of the related uncertainty contribution individual PRT sensors could not be performed. Instead the mean OBCT temperature, averaged and quality controlled by the data provider was used in the measurement equation.
- For MWHS/1 and MWHS/2, all the quality flags, which are provided in level 1a files could not be used due to limited access to documentation. However, the quality flags provided for the geolocation and time have been used.
- Due to setting a static calibration count threshold, there is the risk that non-physical count outliers are included in the data records. Although, in most cases the additionally applied tests should capture those cases, there is a small risk.

Appendix A

The appendix provides more information on the algorithm and on how the data are processed.

A.1 Additional processing steps

- The solar azimuth angle is computed using pyorbital[2];
- By applying the Allan deviation on "raw" calibration counts over 300 scanline a first guess indicator of the calibration count variation is obtained (used in section 3.7);
- The impact of the moon on DSV counts evaluated and three moon flags are computed: 1) moon is close, but not significant; 2) at least 1 DSV count is contaminated; 3) all DSV counts are contaminated by the moon;
- Decode or extract the warm and cold target temperature bias and the non-linearity coefficient and interpolate them to the instrument temperature (see section 3.3);
- Compute the antenna viewing position and compare it to the position, reported in the input file. In case of differences larger than a predefined threshold, these FOVs are flagged.

A.2 Providing quality flags

The quality flags in the output file are compiled from quality flags read from the input file and those, which are collected during the processing.

The content of quality information, given in the input file vary strongly between the instrument and data provider. Hence, not for all instruments, the same density of quality information is provided. The quality flags, which are considered from the input files, are introduced in Table 8. If the quality information is not available, or the interpretation of a given quality flag is suspicious, a zero is provided, meaning this flag is not set. In the current version, the quality-flagging concept is preserved from the FIDUCEO project.

Table 8 List of quality flags from the level 1a files and their availability per instrument. The naming of the flags is determined from the MHS NOAA level 1b file. If a quality flag is used, the name is included in the table, which refer to the list in the text.

Quality flag from L1A	ATMS	MHS	MWHS
qualbit_badtimefieldbutinferrable	✗	✓	✗
qualbit_badtimefield	ATMS_QF_1	✓	MWHS_QF_1
qualbit_general_timeseqErr	ATMS_QF_2	✓	✗
qualbit_earth_notEarthloc	ATMS_QF_2	✓	✗
qualbit_inconstisttime	✗	✓	✗
qualbit_repeatedscantimes	✗	✓	✗
qualbit_general_noEarthloc	ATMS_QF_2	✓	MWHS_QF_2
qualbit_general_noCalib_insuffdata	ATMS_QF_2	✓	MWHS_QF_3
qualbit_earth_questTimecode	ATMS_QF_2	✓	✗
qualbit_earth_margagree	ATMS_QF_2	✓	✗
qualbit_earth_fail	ATMS_QF_2	✓	✗
STX1_status	ATMS_QF_3	✓	✗
STX2_status	ATMS_QF_3	✓	✗
STX3_status	ATMS_QF_3	✓	✗

[2] http://pytroll.github.io

Quality flag from L1A	ATMS	MHS	MWHS
STX4_status	ATMS_QF_3	✓	✗
SARRA_power	ATMS_QF_3	✓	✗
SARRB_power	ATMS_QF_3	✓	✗

For the NASA JPL level 1a data for ATMS three quality flags have been identified, representing the quality information required by the software:

ATMS_QF_1. From "sci_err_status", bit 2/3 (Time Error)
ATMS_QF_2. From "geo_qual", bit 4 and 8 (Failed geolocation on Earth geoid, 'Failed geolocation of some bands')
ATMS_QF_3. From "sci_err_status", bit 5-8 (SDE Telemetry/Header Parity Error, ESF reflector position unavailable, and ESF - SDE command transmit time out)

For MHS, all quality flags are available from the NOAA level 1b file format.

For MWHS less quality flags are available and the documentation is rare. Thus, it is not possible to interpret the available quality flags with sufficient certainty. Only those, which can be interpreted, are used. These are also partly used within the AAPP processing (See RD1). These are:

MWHS_QF_1. From GROUP_TABLE/Time Vdata, Quality_Flag_for_Time_Data
MWHS_QF_2. From GROUP_TABLE/Quality Indicator Vdata,GeoLocation_Quality_Flag
MWHS_QF_3. Quality check on the calibration view angles (as performed by AAPP)

These quality flags are combined with those computed in the processing and compiled to four quality flags that are provided in the level 1c output file. Below those quality flags are introduced, while a more comprehensive explanation is given in the product user guide [RD3], supporting the user to apply these flags best for its specific use.

- data_quality_bitmask, [across track ; along track]
  - summarises any issue related to the calibration target, such as moon intrusion or bad PRT measurements

- quality_issue_pixel_bitmask [across track ; along track; channel]
  - summarises any issue related to the calibration target measurement or earth view measurement, such as no sufficient number of valid calibration counts

- quality_pixel_bitmask [across track ; along track]
  - summarises any issue related to the input data and the geolocation, such as invalid geolocation, invalid time variable, or if the input data are flagged

- quality_scanline_bitmask [across track ; along track]
  - Summarises any issue related to the transmission of the data. These information are fully taken from the input files as described above. There are no known information in the source files for MWHS/1 and MWHS/2, so for those instruments this bitmask is always equal zero.

A.3 Format for MHS

Dimensions:
TempDatDim, calibview, channel, n_Qflags, oscillator, prtcalibs, scanpos, time

Coordinates:

scanpos	(scanpos)	1 2 3 4 5 6 7 ...
channel	(channel)	1 2 3 4 5
prtcalibs	(prtcalibs)	1 2 3
TempDatDim	(TempDatDim)	1 2 3 4 5 6 ...
Oscillator	(oscillator)	1 2
n_Qflags	(n_Qflags)	1 2 3 4 5 6 7 ...
calibview	(calibview)	1 2 3 4
time	(time)	datetime64[ns]
scanline	(time)	291 292 293 294
lon	(time, scanpos)	
lat	(time, scanpos)	

Data variables:

Latitude	(time, scanpos)	float64
quality_flags_bitfield	(time)	uint32
PRT_counts	(time, channel)	float32
OBCT_view	(time, calibview, channel)	float64
Scnlinf	(time)	float32
LunarAngles	(time, calibview)	float64
Longitude	(time, scanpos)	float64
scanline_number	(time)	float32
AntennaPositionConversionFactor	(time, oscillator)	float32
PRT_CALIB	(time, prtcalibs)	float32
majorframe_count	(time)	float32
solar_zenith_angle	(time, scanpos)	float32
PIE_ID	(time, channel)	float64
SPACE_view_mid_pixel_position	(time, calibview)	float32
LO_nonlinearity_coeff	(time, oscillator, channel, prtcalibs)	float32
ColdSpaceCorrectionFactor	(time, channel, prtcalibs)	float32
Qflags_data	(time, n_Qflags)	float32
platform_zenith_angle	(time, scanpos)	float32
relative_azimuth_angle	(time, scanpos)	float32
clockdrift	(time)	float32
OBCT_view_mid_pixel_position	(time, calibview)	float32
Scnlintime	(time)	float64
toa_outgoing_radiance_per_unit_frequency	(time, scanpos, channel)	float32
earth_view_mid_pixel_position	(time, scanpos)	float32
toa_brightness_temperature	(time, scanpos, channel)	float32
year	(time)	float32
Raw_DN_Data	(time, scanpos, channel)	float32
ReferenceTemperature	(time, prtcalibs)	float32
WarmLoadCorrectionFactor	(time, channel, prtcalibs)	float32
TempRadConversion	(time, channel, prtcalibs)	float32
SPACE_view	(time, calibview, channel)	float64
Doy	(time)	float32
ThermTempCoeff	(time, channel)	float32
TemperatureData	(time, TempDatDim)	float64
PRT_TEMP	(time, channel)	float32
platform_altitude	(time)	float32
GranuleFileName	(time)	

Attributes:

A.4 Format for MWHS

Dimensions:

CALIB_target, antenna_coeff, calibview, channel, channel_true, coeff_num, itemp, prtcalibs, prts, scanpos, time

Coordinates:

Channel	(channel)	5.0036 5.0036 6.1147 6.1147 6.1147
channel_true	(channel_true)	1 2 3 4 5
prt_count	(prts)	1 2 3 4 5 6 7 8 9 10
CALIB_target	(CALIB_target)	1 2
Prtcalibs	(prtcalibs)	1 2
space_view_angle	(calibview)	106.9 107.1 107.3
black_body_view_angle	(calibview)	359.8 0.0 0.25
inst_temp_for_nl	(itemp)	1 2 3 4
nl_coeff_number	(coeff_num)	1 2 3
r_s_coeff	(antenna_coeff)	1 2
longitude	(time, scanpos)	
latitude	(time, scanpos)	
time	(time)	datetime64[ns]

Data variables:

Earth_Obs_BT	(time, scanpos, channel_true)	float64
Raw_DN_Data	(time, scanpos, channel)	float32
Lat	(time, scanpos)	float64
lon	(time, scanpos)	float64
solar_zenith_angle	(time, scanpos)	float32
solar_azimuth_angle	(time, scanpos)	float32
platform_zenith_angle	(time, scanpos)	float32
platform_azimuth_angle	(time, scanpos)	float32
Inst_Temp	(time, CALIB_target)	float32
SPACE_view	(time, calibview, channel)	float32
OBCT_view	(time, calibview, channel)	float32
PRT_TEMP_AVE	(time, prtcalibs)	float64
PRT_counts	(time, prts)	float32
PRT_TEMP	(time, prts)	float64
LunarAngles	(time)	float64
Black_Body_View_Ang	(time, calibview)	float32
Space_View_Ang	(time, calibview)	float32
Pixel_View_Angle	(time, scanpos)	float32
pixel_qc	(time, scanpos)	float32
cal_qc	(time)	float32
scnlin_qc	(time)	float64
relative_azimuth_angle	(time, scanpos)	float32
Antenna_Correction	(time, scanpos, channel, antenna_coeff)	float32
Ref_Temp	(time, channel, itemp)	float32
Calibration_Quality_Flag	(time)	int16
GeoLocation_Quality_Flag	(time)	int16
DPPS_Quality_Flag	(time)	int32
GranuleFileName	(time)	string
OrbitNumber	(time)	uint32
OrbitPeriod	(time)	uint16
Quality_Flag_for_Time_Data	(time)	int16
satellite_altitude	(time)	float64
geolocation_Qflag_AAPP	(time, scanpos)	float64
TIME_Qflag_AAPP	(time)	float64
SCANLINE_NUMBER_PACKAGE	(time)	int64
scanline_number	(time)	float64

Attributes:

Chs_Central_Wavenumber, Warm Target Fixed Bias, Cold Space Fixed bias, Altitude, PRT count conversion, nonlinearity_uval, u_nonlinearity_uval, altitude, Nonlinearity, u_nonlinearity, bandcorr_b, bandcorr_a, bandcorr_a_s, bandcorr_b_s, warm_count_thresholds, space_count_thresholds, earth_view_count_thresholds, max_count_jump_between_scanlines, calib_max_count_jump, earth_max_count_jump, jump_thrICTtempmean, space_view_angles, black_body_view_angles, a0FOV_earth, FOV_earth

A.5 Format for ATMS

Dimensions:

bb_count, calibview, channel, engtrack, prts, ref_temp, scanpos, shelf_prt, time

Coordinates:

channel	(channel)	18 19 20 21 22
shelf_prt	(shelf_prt)	4
ref_temp	(ref_temp)	-10 5 20
time	(time)	datetime64[ns]
latitude	(time, scanpos)	44.615753 44.85829 ...
longitude	(time, scanpos)	106.21674 105.45694 ...
sat_alt	(time)	833473.56 833335.75 833300.44 ...
earth_view_angle	(time, scanpos)	-52.72888 -51.619263 ...
view_angle	(time, scanpos)	52.597713 51.49006 ...
space_view_angle	(time, calibview)	81.727295 82.787476 ...
black_body_view_angle	(time, calibview)	

Data variables:

scanline_number	time)	int64
lat	(time, scanpos)	float32
lon	(time, scanpos)	float32
solar_zenith_angle	(time, scanpos)	float32
solar_azimuth_angle	(time, scanpos)	float32
platform_zenith_angle	(time, scanpos)	float32
platform_azimuth_angle	(time, scanpos)	float32
relative_azimuth_angle	(time, scanpos)	float32
LunarAngles	(time, calibview)	float32
Black_Body_View_Ang	(time, calibview)	float32
Space_View_Ang	(time, calibview)	float32
Pixel_View_Angle	(time, scanpos)	float32
Raw_DN_Data	(time, scanpos, channel)	float32
SPACE_view	(time, calibview, channel)	float32
OBCT_view	(time, calibview, channel)	float32
PRT_ref_res	(time, bb_count)	uint16
PRT_TEMP	(time, prts)	float32
hk_2w_res1	(time, engtrack)	uint16
hk_2w_res2	(time, engtrack)	uint16
two_wire_gnd	(time, engtrack)	uint16
four_wire_gnd	(time, engtrack)	uint16
Inst_Temp	(time, shelf_prt)	float32
Antenna_Correction	(time, channel, scanpos)	float64
GranuleFileName	(time)	
inst_state	(time, scanpos)	uint8
geo_qual	(time, scanpos)	uint16
sci_err_status	(time, scanpos)	uint8
sci_status_code	(time, scanpos)	uint8
bb_inst_state	(time, calibview)	uint8
bb_err_status	(time, calibview)	uint8
bb_status_code	(time, calibview)	uint8
space_inst_state	(time, calibview)	uint8
space_err_status	(time, calibview)	uint8
space_status_code	(time, calibview)	uint8
sd_mode_err	(time, engtrack)	uint16
inst_mode	(time, engtrack)	uint16
err_status	(time, engtrack)	uint16

Attributes:

Altitude, Chs_Central_Wavenumber, Warm_Target_Fixed_Bias, Cold_Space_Fixed_bias, Nonlinearity_Corr_Coe, shelf_reference_temperature, bandcorr_a, bandcorr_b, bandcorr_a_s, bandcorr_b_s, earth_count_thresh, space_count_thresh, warm_count_thresh, earth_max_count_jump, calib_max_count_jump

ECMWF Shinfield Park Reading RG2 9AX UK